

# A Variable Eddington Factor Model for Thermal Radiative Transfer with Closure based on Data-Driven Shape Function

Joseph M. Coale<sup>a,c</sup>, Dmitriy Y. Anistratov<sup>b,d</sup>

<sup>a</sup>*Computational Physics and Methods Group, Los Alamos National Laboratory, Los Alamos, NM*

<sup>b</sup>*Department of Nuclear Engineering, North Carolina State University, Raleigh, NC*

<sup>c</sup>*jmcoale@lanl.gov*

<sup>d</sup>*anistratov@ncsu.edu*

---

## Abstract

A new variable Eddington factor (VEF) model is presented for nonlinear problems of thermal radiative transfer (TRT). The VEF model is a data-driven one that acts on known (a-priori) radiation-diffusion solutions for material temperatures in the TRT problem. A linear auxiliary problem is constructed for the radiative transfer equation (RTE) with opacities and emission source evaluated at the known material temperatures. The solution to this RTE approximates the specific intensity distribution for the problem in all phase-space and time. It is applied as a shape function to define the Eddington tensor for the presented VEF model. The shape function computed via the auxiliary RTE problem will capture some degree of transport effects within the TRT problem. The VEF moment equations closed with this approximate Eddington tensor will thus carry with them these captured transport effects. In this study, the temperature data comes from multigroup  $P_1$ ,  $P_{1/3}$ , and flux-limited diffusion radiative transfer (RT) models. The proposed VEF model can be interpreted as a transport-corrected diffusion reduced-order model. Numerical results are presented on the Fleck-Cummings test problem which models a supersonic wavefront of radiation. The presented VEF model is shown to reliably improve accuracy by 1-2 orders of magnitude compared to the considered radiation-diffusion model solutions to the TRT problem.

*Keywords:* Boltzmann transport equation, variable Eddington tensor, radiation diffusion, model order reduction, nonlinear PDEs

---

## 1. Introduction

The modeling and simulation of thermal radiation transport is an important consideration for many applications. Such phenomena can be found in a wide array of different fields, including: high-energy density (HED) physics, astrophysics, plasma physics, fire and combustion physics, and atmospheric and ocean sciences [1, 2, 3, 4, 5, 6]. Multiphysical models of these phenomena comprise complex systems of partial differential equations (PDEs) which must be solved by means of numerical simulation. Some challenges are associated with the numerical simulation these systems. The involved equations are characterized by tight coupling, strong nonlinearities and multiscale behavior in space-time.

Since radiative transfer (RT) is an important mechanism for energy redistribution in these phenomena, a photon transport model must be included in the systems of equations to model RT effects. The equations of RT are high-dimensional, their solution typically depending on 7 independent variables in 3D geometry. Thus along with the aforementioned challenges, a massive number of degrees of freedom (DoF) must be used in calculations to adequately describe the overall solution. For a simulation that discretizes each independent variable with an  $x$ -point grid,  $x^7$  DoF are required, making it reasonable to reach trillions or quadrillions of DoF. The resulting computational load and memory occupation can become intractable for large simulations without the use of exascale computing resources.

A common approach to develop models for simulation of RT phenomena in multiphysics problems is to apply methods of dimensionality reduction for the RT component. This will significantly reduce the required computational resources in exchange for some level of approximation and modeling error in the resulting solution. The goal for an RT model is to find balance between computational load with the desired fidelity of solutions. There exist many well-known RT models based on moment equations with approximate closures which have seen extensive use in application, such as  $M_N$  methods that use maximum entropy closure relations, the  $P_1$  and  $P_{1/3}$  models, and flux-limited diffusion models [7, 8, 9, 10, 11, 12]. Variable Eddington factor (VEF) models makeup another such class of RT models [13, 14, 15]. VEF models are constructed by reformulating the radiation pressure tensor in terms of the Eddington tensor which brings closure to the moment equations. There exist many ways to construct approximation for the Eddington tensor. Some commonly used VEF models apply Wilson, Kershaw and Levermore closures [16, 17, 18, 19, 12]. Numerical methods for solving the Boltzmann transport equation have been developed based on the first two angular moment equations with exact closure defined by the Eddington tensor [20, 21, 22, 23, 24].

The anisotropic diffusion (AD) model has been developed for thermal radiative transfer (TRT) and other particle transport applications [25, 26, 27, 28]. A diffusion equation is constructed which is closed by means of an AD coefficient. The AD coefficient is defined via the solution to an auxiliary transport problem which takes the form of an angular and spatially dependent shape function. The special shape function accounts for some degree of transport effects in the TRT problem. This yields the tensor-diffusion moment equations with transport-corrected AD coefficients. The AD model uses just one transport sweep to solve for the auxiliary function.

A new approach based on data-driven reduced-order models (ROMs) has been gaining popularity in recent years which make use of data-based methodologies to dimensionality reduction. Data-driven models have been developed for (i) linear particle transport problems [29, 30, 31, 32, 33, 34, 35, 36, 37, 38, 39, 40, 41, 42, 43, 44, 45, 46, 47, 48] (ii) nonlinear RT problems [49, 50, 51, 52, 53, 54, 55, 56, 57, 58, 59, 60], and (iii) various problems in nuclear reactor-physics [61, 62, 63, 64, 65, 66, 67, 68, 69, 70, 71]. The fundamental idea behind these ROMs is to leverage databases of solutions to their problems of interest (known a-priori) to develop some reduction in the dimensionality for their involved equations. By nature, these models are problem-dependent since they are formulated using chosen datasets, and this allows for higher levels of accuracy than displayed by other types of ROMs (within the

regime of parameters covered by the datasets).

In this paper we present a data-driven VEF model for the fundamental TRT problem. This kind of TRT problem models a supersonic flow of radiation through matter and neglects hydrodynamic motion of the underlying material and heat conduction [72]. Note that the TRT problem is characterized by the same fundamental challenges as the more general class of problems (e.g. radiation-hydrodynamics problems) and serves as a useful computational platform for the development of new models. There exist several pathways to obtain an approximate Eddington tensor by data-driven means if data on the RT solution for a subset of problem parameters can be obtained [53, 55, 58, 59, 60]. For the model developed here, the Eddington tensor is computed from approximate solution data to the TRT problem generated with radiation-diffusion models. It has been previously shown that the solution of the Boltzmann transport equation computed with a scattering source term evaluated by a diffusion solution yields a sufficiently accurate shape function for estimation of the Eddington tensor in linear problems [73, 74]. An extension of this idea to the nonlinear TRT problem is to use the material temperatures evaluated with a radiation-diffusion model to compute the opacity and emission source in the radiative transfer equation (RTE). This step of the new model uses only one transport sweep to calculate a shape function accounting approximately for transport effects, and to generate the Eddington tensor for the TRT problem.

The remainder of the paper is as follows. The TRT problem is described in Sec. 2, along with definitions for several classical moment-based RT models applied to generate data for computation of the auxiliary shape function. The new data-driven VEF model is formulated in Sec. 3. Numerical results are given in Sec. 4, followed by conclusions in Sec. 5.

## 2. Thermal Radiative Transfer and Models Based on Moment Equations

The TRT problem is formulated by the multigroup RTE

$$\frac{1}{c} \frac{\partial I_g}{\partial t} + \boldsymbol{\Omega} \cdot \boldsymbol{\nabla} I_g + \kappa_g(T) I_g = \kappa_g(T) B_g(T), \quad (1a)$$

$$I_g|_{\mathbf{r} \in \partial\Gamma} = I_g^{\text{in}} \quad \text{for } \boldsymbol{\Omega} \cdot \mathbf{n}_\Gamma < 0, \quad I_g|_{t=0} = I_g^0, \quad (1b)$$

$$\mathbf{r} \in \Gamma, \quad t > 0, \quad \boldsymbol{\Omega} \in \mathcal{S}, \quad g = 1, \dots, G,$$

and the material energy balance (MEB) equation

$$\frac{\partial \varepsilon(T)}{\partial t} = \sum_{g=1}^G \left( \int_{4\pi} I_g d\Omega - 4\pi B_g(T) \right) \kappa_g(T), \quad T|_{t=0} = T^0, \quad (2)$$

where  $\mathbf{r}$  is spatial position,  $t$  is time,  $g$  is the frequency group index,  $\Gamma$  is the spatial domain,  $\partial\Gamma$  is the boundary surface of  $\Gamma$ ,  $\mathbf{n}_\Gamma$  is the unit outward normal to  $\partial\Gamma$ ,  $I_g(\mathbf{r}, \boldsymbol{\Omega}, t)$  is the group specific photon intensity,  $T(\mathbf{r}, t)$  is the material temperature,  $\kappa_g(\mathbf{r}, t; T)$  is the group material opacity,  $\varepsilon(\mathbf{r}, t; T)$  is the material energy density, and  $B_g(\mathbf{r}, t; T)$  is the group Planckian function given by

$$B_g(T) = \frac{2}{c^2 h^2} \int_{\nu_{g-1}}^{\nu_g} \frac{\nu^3}{e^{\frac{\nu}{T}} - 1} d\nu. \quad (3)$$

$c$  is the speed of light,  $h$  is Planck's constant,  $\nu$  is photon frequency.

There are several TRT models which apply moment equations for the group radiation energy density

$$E_g = \frac{1}{c} \int_{4\pi} I_g d\Omega, \quad (4)$$

and flux

$$\mathbf{F}_g = \int_{4\pi} \boldsymbol{\Omega} I_g d\Omega, \quad (5)$$

to approximate the RTE. The  $P_1$  model is defined by the multigroup  $P_1$  equations for radiative transfer, given by

$$\frac{\partial E_g}{\partial t} + \boldsymbol{\nabla} \cdot \mathbf{F}_g + c\kappa_g(T)E_g = 4\pi\kappa_g(T)B_g(T), \quad (6a)$$

$$\frac{1}{c} \frac{\partial \mathbf{F}_g}{\partial t} + \frac{c}{3} \boldsymbol{\nabla} E_g + \kappa_g(T) \mathbf{F}_g = 0, \quad (6b)$$

$$\mathbf{F}_g|_{r \in \partial\Gamma} = \frac{1}{2} E_g|_{r \in \partial\Gamma} + 2F_g^{\text{in}}, \quad (6c)$$

$$E_g|_{t=0} = E_g^0, \quad \mathbf{F}_g|_{t=0} = \mathbf{F}_g^0. \quad (6d)$$

The hyperbolic time-dependent  $P_1$  equations are derived from the RTE by taking its 0<sup>th</sup> and 1<sup>st</sup> angular moments. Closure for the moment equations is formulated by defining the highest (2<sup>nd</sup>) angular moment

$$H_g = \int_{4\pi} \boldsymbol{\Omega} \otimes \boldsymbol{\Omega} I_g d\Omega \quad (7)$$

with the expansion

$$I_g = \frac{1}{4\pi} (cE_g + 3\boldsymbol{\Omega} \cdot \mathbf{F}_g). \quad (8)$$

This approximation yields

$$H_g = \frac{c}{3} E. \quad (9)$$

The  $P_{1/3}$  model for radiative transfer is formulated by the balance equation (6a) and the modified first moment equation given by [7, 8]

$$\frac{1}{3c} \frac{\partial \mathbf{F}_g}{\partial t} + \frac{c}{3} \boldsymbol{\nabla} E_g + \kappa_g(T) \mathbf{F}_g = 0, \quad (10)$$

The factor  $\frac{1}{3}$  at the time-derivative term in Eq. (10) produces the correct the propagation speed of radiation in vacuum.

The flux-limited diffusion (FLD) models are defined by the time-dependent multigroup diffusion equations [15, 75, 76, 77, 78]

$$\frac{\partial E_g}{\partial t} + c \boldsymbol{\nabla} \cdot (-D_g \boldsymbol{\nabla} E_g) + c\kappa_g(T)E_g = 4\pi\kappa_g(T)B_g(T), \quad (11a)$$

$$\mathbf{n}_\Gamma \cdot (-cD_g \boldsymbol{\nabla} E_g)|_{r \in \partial\Gamma} = \frac{1}{2} E_g|_{r \in \partial\Gamma} + 2F_g^{\text{in}}, \quad E_g|_{t=0} = E_g^0, \quad (11b)$$

and

$$\mathbf{F}_g = -cD_g \nabla E_g, \quad (12)$$

where  $D_g$  is the group diffusion coefficient. In this model, the time derivative of the flux in the first moment equation is neglected. This leads to a parabolic time-dependent equation for  $E_g$  with the diffusion coefficient defined by

$$D_g = \frac{1}{3\kappa_g(T)}. \quad (13)$$

In general, the solution of the diffusion equation (11a) with  $D_g$  defined by Eq. (13) does not satisfy the flux-limiting condition

$$\frac{|\mathbf{F}_g|}{cE_g} \leq 1, \quad (14)$$

stemming from definitions of the radiation density and flux (Eqs. (4) and (5)). The FLD models introduce modifications of the diffusion coefficient to meet the condition in Eq. (14). In this study, we consider the coefficient proposed by E. Larsen [7]

$$D_g(T, E_g) = \left[ (3\kappa_g(T))^2 + \left( \frac{1}{E_g} \nabla E_g \right)^2 \right]^{\frac{1}{2}}. \quad (15)$$

### 3. Variable Eddington Factor Model for TRT with Diffusion-Based Shape Function

The Variable Eddington factor method is defined by the balance equation (Eq. (6a)) and the first moment equation

$$\frac{1}{c} \frac{\partial \mathbf{F}_g}{\partial t} + c \nabla (\mathfrak{f}_g E_g) + \kappa_g(T) \mathbf{F}_g = 0, \quad (16)$$

where closure is defined with

$$H_g = c \mathfrak{f}_g[\tilde{I}] E_g, \quad (17)$$

by means of the Eddington tensor given as

$$\mathfrak{f}_g[\tilde{I}] = \frac{\int_{4\pi} \boldsymbol{\Omega} \otimes \boldsymbol{\Omega} \tilde{I}_g d\Omega}{\int_{4\pi} \tilde{I}_g d\Omega}. \quad (18)$$

Here  $\tilde{I}_g$  is an approximation of the photon intensity. There exist a group of VEF models which use an approximation of the Eddington tensor defined via the first two moments of the photon intensity [17, 79, 18, 80, 81, 82, 83, 78, 84, 12].

To define the Eddington tensor, we formulate a model in which the material temperature distribution  $\tilde{T}$  for a TRT problem is calculated with one of the radiation-diffusion models

described in Sec. 2. A linear RTE is then defined by available  $\tilde{T}(\mathbf{r}, t)$  for  $t \in [0, t^{\text{end}}]$  and  $\mathbf{r} \in \Gamma$

$$\frac{1}{c} \frac{\partial \tilde{I}_g}{\partial t} + \boldsymbol{\Omega} \cdot \nabla \tilde{I}_g + \kappa_g(\tilde{T}) \tilde{I}_g = \kappa_g(\tilde{T}) B_g(\tilde{T}), \quad (19a)$$

$$\begin{aligned} \tilde{I}_g|_{\mathbf{r} \in \partial\Gamma} &= I_g^{\text{in}} \text{ for } \mathbf{n}_\Gamma \cdot \boldsymbol{\Omega} < 0, & \tilde{I}_g|_{t=t_0} &= I_g^0, \\ \mathbf{r} \in \Gamma, \quad t \in [0, t^{\text{end}}], \quad \boldsymbol{\Omega} \in \mathcal{S}, \quad g &= 1, \dots, G. \end{aligned} \quad (19b)$$

The solution of the auxiliary RTE problem (19) gives an approximate distribution of radiation intensities  $\tilde{I}_g$  which accounts for the transport effects of the TRT problem and can be used as a shape function to compute approximate Eddington tensor (18). The boundary conditions for the VEF moment equations are defined in terms of  $\tilde{I}_g$  as follows [20, 22]:

$$\mathbf{n}_\Gamma \cdot \mathbf{F}_g|_{\mathbf{r} \in \partial\Gamma} = c C_g[\tilde{I}_g](E_g|_{\mathbf{r} \in \partial\Gamma} - E^{\text{in}}) + F_g^{\text{in}}, \quad (20)$$

where

$$C_g[\tilde{I}_g] = \frac{\int_{\mathbf{n}_\Gamma \cdot \boldsymbol{\Omega} > 0} \boldsymbol{\Omega} \tilde{I}_g d\Omega}{\int_{\mathbf{n}_\Gamma \cdot \boldsymbol{\Omega} > 0} \tilde{I}_g d\Omega}. \quad (21)$$

The RTE (19) with the given function of temperature can be efficiently solved with a single transport sweep per time step. To solve the Eqs. (19) ray tracing techniques (aka the method of long characteristics) are applied [85, 86, 87, 88, 89, 90, 91, 92]. In sum, the data-driven VEF model for TRT is constructed with:

- Radiation-diffusion solution data for material temperatures  $\tilde{T}$ ,
- The RTE with opacity and Planckian source evaluated with  $\tilde{T}$  (Eqs. (19)),
- The VEF equations (Eqs. (6a) & (16)), where the Eddington tensor is defined via Eq. (18) and boundary conditions given by Eq. (20).

Hereafter we refer to this model as the data-driven VEF model (DD-VEF).

---

**Algorithm 1:** Offline phase of DD-VEF model

---

Input:  $\{\tilde{T}(t^n)\}_{n=1}^N$   
 $n = 0$   
**while**  $t^n < t^{\text{end}}$  **do**  
     $n = n + 1$   
     $\tilde{T}(t^n) \rightsquigarrow \tilde{I}_g(t^n)$  (Eqs. (19))  
     $\tilde{I}_g(t^n) \rightsquigarrow \tilde{\mathbf{f}}_g(t^n)$  (Eq. (18))  
**end**  
Output:  $\{\tilde{\mathbf{f}}_g(t^n)\}_{n=1}^N$

---

---

**Algorithm 2:** Online phase of DD-VEF model
 

---

Input:  $\{\tilde{\mathbf{f}}_g(t^n)\}_{n=1}^N$   
 $n = 0$   
**while**  $t^n < t^{end}$  **do**  
    $n = n + 1$   
    $\tilde{\mathbf{f}}_g(t^n) \rightsquigarrow \{\mathbf{T}(t^n), \mathbf{E}_g(t^n), \mathcal{F}_g(t^n)\}$  (Eqs. (6a), (16), (20))  
**end**  
 Output:  $\{\mathbf{T}(t^n), \mathbf{E}_g(t^n), \mathcal{F}_g(t^n)\}_{n=1}^N$

---

The process of solving TRT problems with the DD-VEF model can be explained as a two-phase methodology, which is outlined in Algorithms 1 and 2. The first (offline) phase demonstrated by Algorithm 1 represents the ‘data-processing’ operations to prepare the Eddington tensor closure data. The required input is an already known approximate material temperature distribution  $\tilde{T}$  for the entire spatial and temporal interval of interest. If we define a simulation with  $X$  spatial grid cells and  $N$  time steps, then this input data is the set  $\{\tilde{\mathbf{T}}(t^n)\}_{n=1}^N$  where  $\tilde{\mathbf{T}}(t^n) \in \mathbb{R}^X$ . At each  $n^{\text{th}}$  time step, Eq. (19) is solved using  $\tilde{\mathbf{T}}(t^n)$  for the vector of discrete radiation intensities in phase space  $\tilde{\mathbf{I}}_g$ , which give rise to the approximate Eddington tensor on the discrete grid  $\tilde{\mathbf{f}}_g(t^n)$  via Eq. (18). The discrete Eddington tensor values at each time step can be collected and stored in a dataset for later use with the DD-VEF model. This process of preparing the Eddington tensor data is referred to as the offline-phase because it only must be completed once per temperature distribution  $\tilde{T}$ , and the calculated Eddington tensor data can be stored away for later use.

The second (online) phase is outlined in Algorithm 2 and represents the operations required to solve a given TRT problem with the DD-VEF model. Taking as input the Eddington tensor data calculated in Algorithm 1, the DD-VEF equations are solved at each time step to generate vectors for temperature  $\mathbf{T}(t^n)$ , radiation energy densities  $\mathbf{E}_g(t^n)$  and radiation fluxes  $\mathcal{F}_g(t^n)$  over all phase space. In this configuration of offline/online phases, only Algorithm 2 must be completed for any given TRT simulation, assuming Algorithm 1 was completed some time in the past to prepare the required datasets. It is important to note however, that both phases can be combined to save on storage requirements. In this case given the input for  $\{\tilde{\mathbf{T}}(t^n)\}_{n=1}^N$ , at each time step the approximate Eddington tensor is calculated and immediately used with the DD-VEF equations to generate the TRT solution for the time step.

#### 4. Numerical Results

The DD-VEF model is analyzed with numerical testing on the classical Fleck-Cummings (F-C) test [93] in 2D Cartesian geometry. This test takes the form of a homogeneous square domain with sides 6 cm in length, whose material is defined with spectral opacity

$$\kappa_\nu = \frac{27}{\nu^3}(1 - e^{-\nu/T}). \quad (22)$$

Here  $\nu$  and  $T$  are measured in KeV. The left boundary is subject to an isotropic, black-body radiation source at a temperature of  $T^{\text{in}} = 1$  KeV. All other boundaries are vacuum. The initial temperature of the domain is  $T^0 = 1$  eV. The material energy density of the material is a linear one  $\varepsilon = c_v T$  where  $c_v = 0.5917 a_R (T^{\text{in}})^3$ . The problem is solved on the interval  $t \in [0, 6 \text{ ns}]$  with 300 uniform time steps  $\Delta t = 2 \times 10^{-2}$  ns. The phase space is discretized using a  $20 \times 20$  uniform orthogonal spatial grid, 17 frequency groups (see Table 1) and 144 discrete directions. The Abu-Shumays angular quadrature set is used [94]. The implicit backward-Euler time integration scheme is used to discretize all equations in time. The BTE is discretized in space with the method of conservative long characteristics [92], and all low-order equations use a second-order finite-volumes scheme [95].

Note the full-order model (FOM) for this TRT problem is formulated as the RTE coupled with the MEB. Three radiation diffusion models are considered to generate  $\tilde{T}$ : multigroup FLD,  $P_1$  and  $P_{1/3}$  (see Sec. 2). The physics embedded in  $\tilde{T}$  will vary depending on which diffusion type model is used in its computation. For instance the FLD,  $P_1$  and  $P_{1/3}$  models may all produce different propagation speeds (and spectral distributions) of the radiation wavefront [7]. These effects change how energy is redistributed in the F-C test and alters the distribution of material temperatures in space-time.

Table 1: Upper boundaries for each frequency group

|               |        |       |       |       |       |       |       |                 |       |
|---------------|--------|-------|-------|-------|-------|-------|-------|-----------------|-------|
| $g$           | 1      | 2     | 3     | 4     | 5     | 6     | 7     | 8               | 9     |
| $\nu_g$ [KeV] | 0.7075 | 1.415 | 2.123 | 2.830 | 3.538 | 4.245 | 5.129 | 6.014           | 6.898 |
| $g$           | 10     | 11    | 12    | 13    | 14    | 15    | 16    | 17              |       |
| $\nu_g$ [KeV] | 7.783  | 8.667 | 9.551 | 10.44 | 11.32 | 12.20 | 13.09 | $1 \times 10^7$ |       |

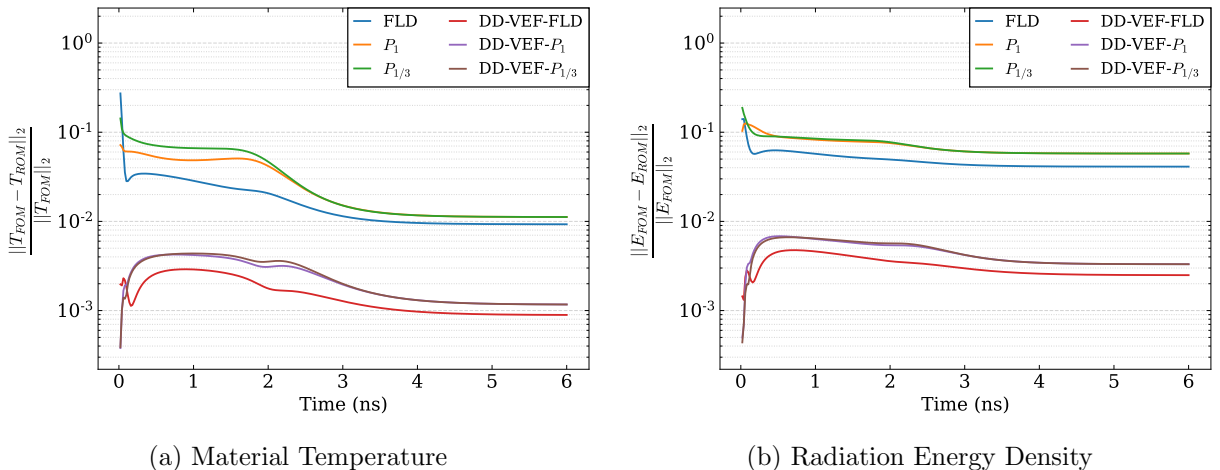


Figure 1: Relative errors in the 2-norm for  $\tilde{T}$ ,  $\tilde{E}$  produced by the FLD,  $P_1$  and  $P_{1/3}$  models, and for  $T$ ,  $E$  found with the DD-VEF model generated using each  $\tilde{T}$ , plotted vs time. Errors are calculated vs the FOM.

Figure 1 plots relative errors (w.r.t. the FOM solution) for the material temperature and total radiation energy density calculated in the 2-norm over space at each instant of time in  $t \in [0, 6 \text{ ns}]$ . Separate curves are shown for each considered diffusion model and for the DD-VEF model. In each case the DD-VEF solution finds an increase in accuracy for  $T$  and  $E$  compared to the radiation diffusion solutions. The errors in  $T$  and  $E$  from the DD-VEF model are on the order of  $10^{-3}$  for the whole interval of time, whereas the diffusion model errors exist on order  $10^{-2}$  for the majority of times. The DD-VEF model is seen to increase the accuracy of each diffusion model by roughly an order of magnitude. The FLD model possesses the highest accuracy of all tested diffusion ROMs, and the DD-VEF model with highest accuracy is the one applied to the FLD solution.

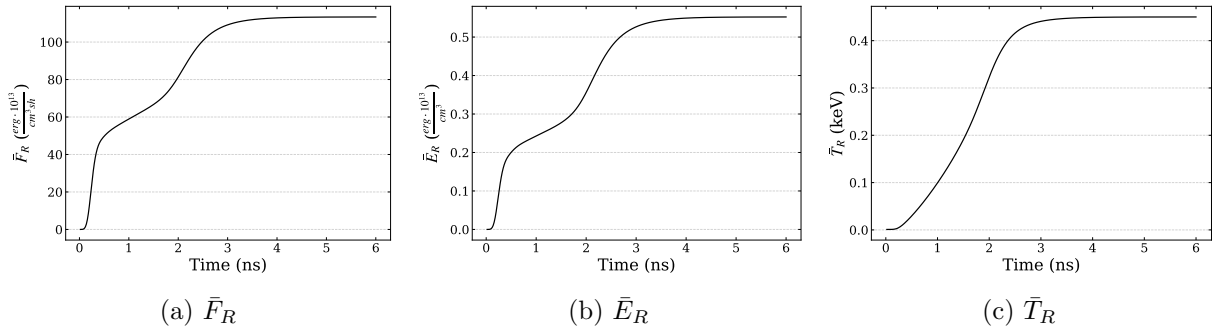


Figure 2: FOM solution for data located at and integrated over the right boundary of the domain.

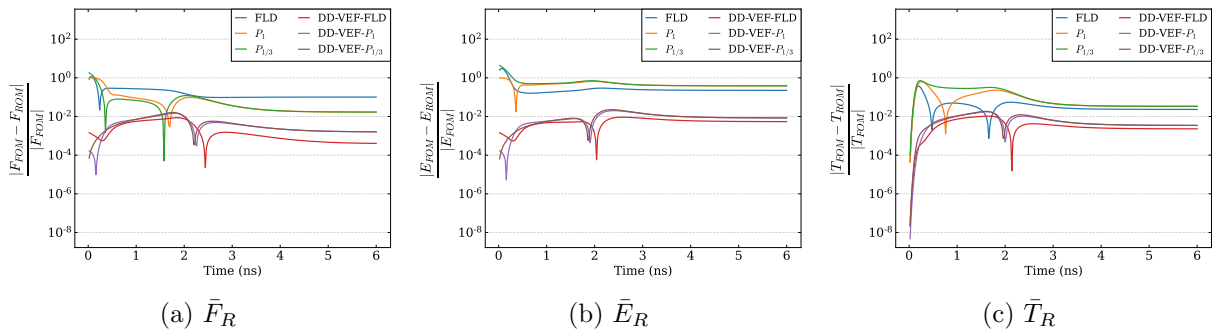


Figure 3: Relative error for the FLD,  $P_1$  and  $P_{1/3}$  models, and the DD-VEF model generated with each diffusion model solution, for data located at and integrated over the right boundary of the domain.

Next we investigate the DD-VEF model's performance in capturing the radiation wavefront as it propagates through the spatial domain. Note that the F-C test mimics the class of supersonic radiation shock problems and experiments [72, 96, 97, 98]. One measurement of importance in these experiments concerns the time it takes for the radiation wavefront to reach the radiation-drive-opposite side of the test material [72, 97, 98]. A measurement of accuracy based on this wavefront-arrival metric can be derived by comparing the TRT solution at the right boundary of the F-C test, where the radiation wavefront propagates towards. The boundary-averaged material temperatures and radiation energy density and

flux are defined as

$$\bar{F}_R = \frac{1}{L_R} \int_0^{L_R} \mathbf{e}_x \cdot \mathbf{F}(x_R, y) dy, \quad (23)$$

$$\bar{E}_R = \frac{1}{L_R} \int_0^{L_R} E(x_R, y) dy, \quad (24)$$

$$\bar{T}_R = \frac{1}{L_R} \int_0^{L_R} T(x_R, y) dy, \quad (25)$$

where  $L_R = x_R = 6\text{cm}$ . The FOM solution for these three quantities vs time is plotted in Figure 2. If the DD-VEF model can reproduce these integral quantities to acceptable levels of accuracy, they can be said to correctly reproduce the shape and propagation speed of the radiation wavefront. This is especially important to investigate given that the considered radiation diffusion models are known to produce nonphysical effects [7, 8, 9]. Figure 3 plots the relative error of the diffusion and DD-VEF produced values of  $\bar{F}_R$ ,  $\bar{E}_R$  and  $\bar{T}_R$ . The relative errors for each quantity are decreased using the DD-VEF model by 1-2 orders of magnitude for most instances of time. There are several time intervals where the errors for a model ‘spike’ downwards and then come back up. These occur when there is a change of sign in the error and do not indicate that the solution is more accurate there than at other instants of time. The most dramatic increase in accuracy is for the FLD  $\bar{F}_R$  by about 3 orders of magnitude. In fact, the FLD  $\bar{F}_R$  is the least accurate and the DD-VEF model  $\bar{F}_R$  using the FLD solution is the most accurate of the models shown. The explanation for this effect comes from the fact that the DD-VEF model only acts on the approximate material temperature it is given, and the FLD solution for  $\bar{T}_R$  (and  $T$  in general from Figure 1) is the most accurate of the considered radiation diffusion models.

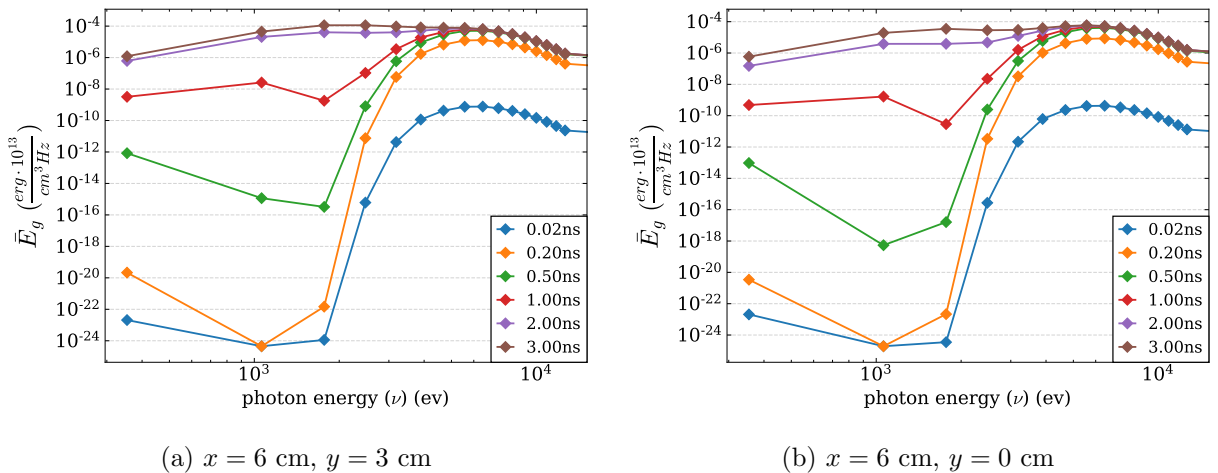


Figure 4: Radiation energy density spectrum located at two points on the right boundary of the domain of the F-C test, taken at several time instances.

Finally, we consider the spectrum of radiation present on the right boundary of the test domain. Figure 4 plots the frequency spectrum of radiation energy densities for the F-C test obtained by FOM on two points of the right boundary face ( $x = 6$  cm). The spectrum of radiation present at the midpoint of the right boundary ( $y = 3$  cm) is shown on the left, and the radiation spectrum present at the corner of the test domain ( $y = 0$  cm) is displayed on the right. Select instants of time are plotted to demonstrate how the radiation spectrum evolves. The points on the graphs are located at the center of each discrete energy group on the frequency-axis, and the values they take on are the group-averaged radiation energy densities  $\bar{E}_g = E_g/(\nu_g - \nu_{g-1})$ . The plots have been ‘zoomed in’ to the spectrum peak, which leaves off the final frequency group. However, this point does not deviate significantly from the position of the second to last frequency group.

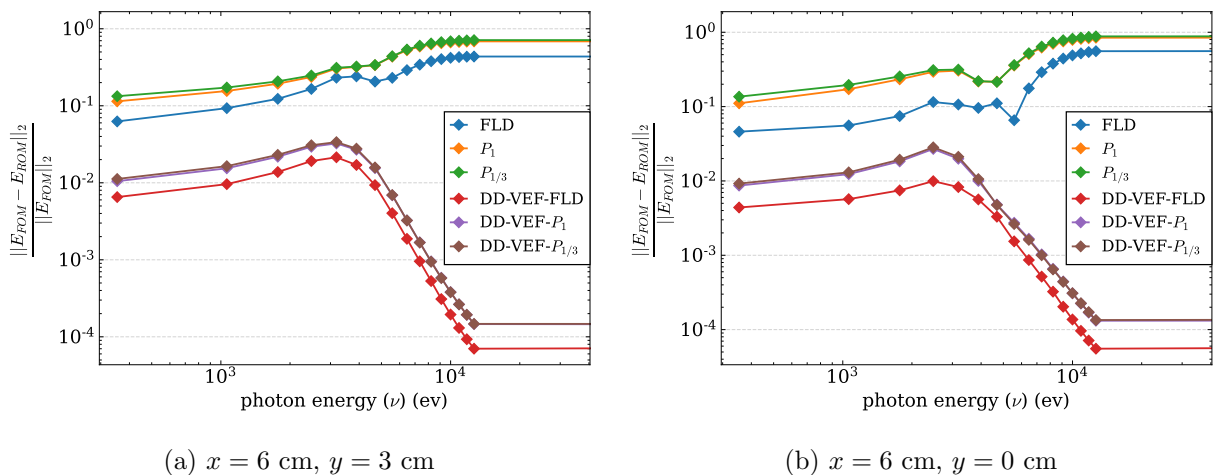


Figure 5: Relative errors of the radiation spectrum located at the midpoint of the right boundary in the temporal 2-norm

Figure 5 plots the errors of each model in the radiation energy densities vs photon frequency at the midpoint of the right boundary. Errors have been collected in the relative *temporal* 2-norms

$$\|x(t)\|_2^t = \left( \int_0^{t^{\text{end}}} x(t)^2 dt \right)^{-1/2}, \quad (26)$$

w.r.t. the full-order solution. The DD-VEF model is demonstrated to improve upon low-frequency group errors by roughly an order of magnitude at each considered point in space. The increase in accuracy from the diffusion solutions significantly improves as frequency increases starting from roughly  $\nu = 3$  KeV. This is where the peak of (non-local) radiation emanating from the boundary drive should be located in frequency, as the Planckian spectrum peaks at  $\nu = 2.82T$ . This makes sense, since the higher frequency groups are closer to the streaming regime and should be better approximated by the transport-effects correction provided within the VEF model. The same errors calculated in the  $\infty$ -norm are close to those shown in the 2-norm, indicating that these results well represent the overall

errors produced by these models in the radiation spectrum at all instants of time. Note that although the last frequency group has not been included in the plots, its error value is close to that of the last shown frequency group for all models.

## 5. Conclusion

In this paper a data-driven VEF model is introduced for nonlinear TRT problems. An approximate Eddington tensor is constructed with a transport correction method applied to radiation diffusion-based solutions to the TRT problem. Three multigroup diffusion models were considered: a FLD model, and the  $P_1$ ,  $P_{1/3}$  models. The DD-VEF model provided an increase in accuracy of 1-2 orders of magnitude in the total radiation energy density and material temperature when applied to each diffusion-based solution. The entire spectrum of radiation present at the test domain right boundary was improved upon as well. The most significant reduction in error from the diffusion solutions in the frequency spectrum was in the high-frequency range with strong transport effects. Possible future extensions of this DD-VEF model include parameterization via interpolation between diffusion solutions for a series of TRT problems, or the use of other approximate models for TRT in place of radiation-diffusion.

## 6. Acknowledgements

Los Alamos Report LA-UR-23-31255. This research project was funded by the Sandia National Laboratory, Light Speed Grand Challenge, LDRD, Strong Shock Thrust. This work was supported by the U.S. Department of Energy through the Los Alamos National Laboratory. Los Alamos National Laboratory is operated by Triad National Security, LLC, for the National Nuclear Security Administration of U.S. Department of Energy (Contract No. 89233218CNA000001). The content of the information does not necessarily reflect the position or the policy of the federal government, and no official endorsement should be inferred.

## References

- [1] Y. B. Zeldovich, Y. P. Razier, *Physics of Shock Waves and High Temperature Hydrodynamic Phenomena*, Academic, New York, 1966.
- [2] D. Mihalas, B. Weibel-Mihalas, *Foundation of Radiation Hydrodynamics*, Oxford University Press, 1984.
- [3] F. H. Shu, *The physics of astrophysics*, University Science Books, 1991.
- [4] G. E. Thomas, K. Stamnes, *Radiative Transfer in the Atmosphere and Ocean*, Cambridge, 1999.
- [5] M. Faghri, B. Sundén, *Transport Phenomena in Fires*, volume 20 of *Developments in Heat Transfer*, WIT, 2008.
- [6] R. P. Drake, *High-Energy-Density-Physics: Foundation of Inertial Fusion and Experimental Astrophysics*, Springer, 2018.
- [7] G. L. Olson, L. H. Auer and M. L. Hall, Diffusion,  $P_1$ , and other approximate forms of radiation transport, *Journal of Quantitative Spectroscopy & Radiative Transfer* 64 (2000) 619–634.
- [8] J. E. Morel, Diffusion-limit asymptotics of the transport equation, the  $P_{1/3}$  equations, and two flux-limited diffusion theories, *Journal of Quantitative Spectroscopy & Radiative Transfer* 65 (2000) 769–778.

- [9] K. H. Simmons, D. Mihalas, A linearized analysis of the modified  $P_1$  equations, *Journal of Quantitative Spectroscopy & Radiative Transfer* 66 (2000) 263–269.
- [10] C. D. Hauck, High-order entropy-based closures for linear transport in slab geometry, *Communications in Mathematical Sciences* 9 (2011) 187–205.
- [11] G. W. Alldredge, C. D. Hauck, A. L. Tits, High-order entropy-based closures for linear transport in slab geometry II: A computational study of the optimization problem, *SIAM Journal on Scientific Computing* 34 (2012) B361–B391.
- [12] E. M. Murchikova, E. Abdikamalov, T. Urbatsch, Analytic closures for M1 neutrino transport, *Monthly Notices of the Royal Astronomical Society* 469 (2017) 1725–1737.
- [13] A. Eddington, *The Internal Constitution of the Stars*, Dover, New York, 1926.
- [14] G. C. Pomraning, An extension of the eddington approximation, *J. Quant. Spectrosc. Radiat. Transfer* 9 (1969) 407–422.
- [15] C. D. Levermore, G. C. Pomraning, A flux-limited diffusion theory, *The Astrophysical Journal* 248 (1981) 321–334.
- [16] J. M. LeBlanc, J. R. Wilson, Analytic closures for m1 neutrino transport, *The Astrophysical Journal* 161 (1970) 541–551.
- [17] D. S. Kershaw, Flux limiting nature’s own way – A new method for numerical solution of the transport equation, Technical Report, Lawrence Livermore National Laboratory, Livermore, CA, 1976.
- [18] C. D. Levermore, Relating Eddington factors to flux limiters, *Journal of Quantitative Spectroscopy & Radiative Transfer* 31 (1984) 149–160.
- [19] C. D. Levermore, Moment closure hierarchies for kinetic theories, *Journal of Statistical Physics* 83 (1996) 1021–1065.
- [20] V. Ya. Gol’din, A quasi-diffusion method of solving the kinetic equation, *USSR Comp. Math. and Math. Phys.* 4 (1964) 136–149.
- [21] L. H. Auer, D. Mihalas, On the use of variable Eddington factors in non-LTE stellar atmospheres computations, *Monthly Notices of the Royal Astronomical Society* 149 (1970) 65–74.
- [22] V. Ya. Gol’din, B. N. Chetverushkin, Methods of solving one-dimensional problems of radiation gas dynamics, *USSR Comp. Math. and Math. Phys.* 12 (1972) 177–189.
- [23] V. Ya. Gol’din, D. A. Gol’dina, A. V. Kolpakov, A. V. Shilkov, Mathematical modeling of hydrodynamics processes with high-energy density radiation, *Problems of Atomic Sci. & Eng.: Methods and Codes for Numerical Solution of Math. Physics Problems* 2 (1986) 59–88. In Russian.
- [24] K.-H. A. Winkler, M. L. Norman and D. Mihalas, Implicit adaptive-grid radiation hydrodynamics, in: *Multiple Time Scales*, Academic Press, 1985, pp. 145–184.
- [25] T. J. Trahan, E. W. Larsen, 2-d anisotropic diffusion in optically thin channels, *Transactions of American Nuclear Society* 101 (2009) 387–389.
- [26] S. R. Johnson, E. W. Larsen, An anisotropic diffusion approximation to thermal radiative transfer, in: *Proc. of Int. Conf. on Mathematics and Computational Methods Applied to Nuclear Science and Engineering (M&C 2011)*, Rio de Janeiro, RJ, Brazil, 2011, p. 10 pp.
- [27] T. J. Trahan, E. W. Larsen, 3-d anisotropic diffusion in optically thick media with optically thin channels, in: *Proc. of Int. Conf. on Mathematics and Computational Methods Applied to Nuclear Science and Engineering (M&C 2011)*, Rio de Janeiro, RJ, Brazil, 2011, p. 10 pp.
- [28] S. R. Johnson, E. W. Larsen, Boundary conditions for the anisotropic diffusion approximation, *Transactions of American Nuclear Society* 105 (2011) 443–445.
- [29] A. G. Buchan, A. A. Calloo, M. G. Goffin, S. Dargaville, F. Fang, C. C. Pain, I. M. Navon, A POD reduced order model for resolving angular direction in neutron/photon transport problems, *Journal of Computational Physics* 296 (2015) 138–157.
- [30] J. Tencer, K. Carlberg, M. Larsen, R. Hogan, Accelerated solution of discrete Ordinates approximation to the Boltzmann transport equation for a gray absorbing-emitting medium via model reduction, *Journal of Heat Transfer* 139 (2017) 122701.
- [31] L. Soucasse, A. G. Buchan, S. Dargaville and C. C. Pain, An angular reduced order model for radiative transfer in non grey media, *Journal of Quantitative Spectroscopy & Radiative Transfer* 229 (2019)

- 23–32.
- [32] P. A. Behne, J. C. Ragusa and J. E. Morel, Model order reduction for  $S_N$  radiation transport, in: Proc. of Int. Conf. on Mathematics and Computational Methods Applied to Nuclear Science and Engineering (M&C 2019), 2019, p. 10 pp.
  - [33] Z. K. Hardy, J. E. Morel and C. Ahrens, Dynamic mode decomposition for subcritical metal systems, in: Proc. of Int. Conf. on Mathematics and Computational Methods Applied to Nuclear Science and Engineering (M&C 2019), 2019, p. 10 pp.
  - [34] Z. M. Prince and J. C. Ragusa, Proper generalized decomposition of multigroup neutron diffusion with separated space-energy representation, in: Proc. of Int. Conf. on Mathematics and Computational Methods Applied to Nuclear Science and Engineering (M&C 2019), 2019, p. 10 pp.
  - [35] Z. M. Prince and J. C. Ragusa, Separated representation of spatial dimensions in  $S_N$  neutron transport using the proper generalized decomposition, in: Proc. of Int. Conf. on Mathematics and Computational Methods Applied to Nuclear Science and Engineering (M&C 2019), 2019, p. 10 pp.
  - [36] K. A. Dominesey, W. Ji, Reduced-order modeling of neutron transport separated in space and angle via proper generalized decomposition, in: Proc. of Int. Conf. on Mathematics and Computational Methods Applied to Nuclear Science and Engineering (M&C 2019), 2019, p. 10 pp.
  - [37] Z. Peng, R. G. McClarren and M. Frank, A low-rank method for time-dependent transport calculations, in: Proc. of Int. Conf. on Mathematics and Computational Methods Applied to Nuclear Science and Engineering (M&C 2019), 2019, p. 10 pp.
  - [38] Z. Peng, R. McClarren, A high-order / low-order (HOLO) algorithm with low-rank evolution for time-dependent transport calculations, Transactions of the American Nuclear Society 121 (2019) 805–807.
  - [39] M. M. Pozulp, 1D transport using neural nets,  $S_N$ , and MC, in: Proc. of Int. Conf. on Mathematics and Computational Methods Applied to Nuclear Science and Engineering (M&C 2019), 2019, p. 10 pp.
  - [40] Z. Peng, R. G. McClarren and M. Frank, A low-rank method for two-dimensional time-dependent radiation transport calculations, Journal of Computational Physics 421 (2020) 109735.
  - [41] M. M. Pozulp, P. S. Brantley, T. S. Palmer, J. L. Vujic, Heterogeneity, hyperparameters, and GPUs: Towards useful transport calculations using neural networks, in: Proc. of Int. Conf. on Mathematics and Computational Methods Applied to Nuclear Science and Engineering (M&C 2021), 2021, p. 10 pp.
  - [42] Z. Peng and R. G. McClarren, A low-rank method for the discrete ordinate transport equation compatible with transport sweeps, in: Proc. of Int. Conf. on Mathematics and Computational Methods Applied to Nuclear Science and Engineering (M&C 2021), 2021, p. 10 pp.
  - [43] P. Behne, J. C. Ragusa, M. Tano, Projection-based parametric model order reduction for transport simulation based on affine decomposition of the operators, in: Proc. of Int. Conf. on Mathematics and Computational Methods Applied to Nuclear Science and Engineering (M&C 2021), 2021, p. 10 pp.
  - [44] Y. Choi, P. Brown, W. Arrighi, R. Anderson and K. Huynh, Space-time reduced order model for large-scale linear dynamical systems with application to Boltzmann transport problems, Journal of Computational Physics 424 (2021).
  - [45] M. H. Elhareef, Z. Wu, Y. Ma, Physics-informed deep learning neural network solution to the neutron diffusion model, in: Proc. of Int. Conf. on Mathematics and Computational Methods Applied to Nuclear Science and Engineering (M&C 2021), 2021, p. 10 pp.
  - [46] Z. Peng, Y. Chen, Y. Cheng, F. Li, A reduced basis method for radiative transfer equation, Journal of Scientific Computing 91 (2022).
  - [47] A. C. Hughes, A. G. Buchan, An adaptive reduced order model for the angular discretisation of the Boltzmann transport equation using independent basis sets over a partitioning of the space-angle domain, International Journal for Numerical Methods in Engineering (2022) 1–19.
  - [48] Z. Huang, Y. Chen, A. Christlieb, L. Roberts, Machine learning moment closure models for the radiative transfer equation I: directly learning a gradient based closure, Journal of Computational Physics 453 (2022) 110941.
  - [49] R. Pinnau, A. Schulze, Model reduction techniques for frequency averaging in radiative heat transfer, Journal of Computational Physics 226 (2007) 712–731.
  - [50] J. Qian, Y. Wang, H. Song, K. Pant, Projection-based reduced-order modeling for spacecraft thermal

- analysis, *Journal of Spacecraft and Rockets* 52 (2015) 978–989.
- [51] L. Fagiano, R. Gati, On the order reduction of the radiative heat transfer model for the simulation of plasma arcs in switchgear devices, *Journal of Quantitative Spectroscopy & Radiative Transfer* 169 (2016) 58–78.
  - [52] A. L. Alberti, T. S. Palmer, Reduced order modeling of non-linear radiation diffusion via proper generalized decomposition, *Transactions of the American Nuclear Society* 119 (2018) 691–694.
  - [53] J. M. Coale, D. Y. Anistratov, A reduced-order model for thermal radiative transfer problems based on multilevel quasidiffusion method, in: *Proc. of Int. Conf. on Mathematics and Computational Methods Applied to Nuclear Science and Engineering (M&C 2019)*, Portland, OR, 2019, p. 10 pp.
  - [54] J. M. Coale, D. Y. Anistratov, Data-driven grey reduced-order model for thermal radiative transfer problems based on low-order quasidiffusion equations and proper orthogonal decomposition, *Transactions of the American Nuclear Society* 121 (2019) 836–839.
  - [55] J. M. Coale, D. Y. Anistratov, Reduced-order models for thermal radiative transfer based on POD-Galerkin method and low-order quasidiffusion equations, in: *Proc. of Int. Conf. on Mathematics and Computational Methods Applied to Nuclear Science and Engineering (M&C 2021)*, Raleigh, NC, 2021, p. 10 pp.
  - [56] M. Girault, Y. Liu, Y. Billaud, D. Saury, D. Lemonnier, Reduced order models for conduction and radiation inside sem-transparent media via the model identification method, *International Journal of Heat and Mass Transfer* 168 (2021) 120598.
  - [57] A. L. Alberti, T. S. Palmer, C. J. Palmer, Orthogonal decomposition based reduced-order modeling of flux-limited gray thermal radiation, *Journal of Quantitative Spectroscopy and Radiative Transfer* (2022) 108345.
  - [58] J. M. Coale, D. Y. Anistratov, Reduced order models for thermal radiative transfer problems based on moment equations and data-driven approximations of the eddington tensor, *J. Quant. Spectrosc. Radiat. Transfer* 296 (2023) 108458.
  - [59] J. M. Coale, D. Y. Anistratov, A reduced-order model for thermal radiative transfer problems based on pod-petrov-galerkin projection of the normalized Boltzmann transport equation, in: *Proc. of Int. Conf. on Mathematics and Computational Methods Applied to Nuclear Science and Engineering (M&C 2023)*, Niagara Falls, Ontario, Canada, 2023, p. 10 pp.
  - [60] J. M. Coale, D. Y. Anistratov, A reduced-order model for nonlinear radiative transfer problems based on moment equations and pod-petrov-galerkin projection of the normalized boltzmann transport equation, 2023. Preprint on arXiv:2308.15375, math.NA.
  - [61] A. Cherezov, R. Sanchez and H. G. Joo, A reduced-basis element method for pin-by-pin reactor core calculations in diffusion and  $SP_3$  approximations, *Annals of Nuclear Energy* 116 (2018) 195–209.
  - [62] A. L. Alberti and T. S. Palmer, Reduced order modeling of the twigl problem using proper generalized decomposition, in: *Proc. of Int. Conf. on Mathematics and Computational Methods Applied to Nuclear Science and Engineering (M&C 2019)*, 2019, p. 14 pp.
  - [63] P. German, J. C. Ragusa, C. Fiorina, M. T. Retamales, Reduced-order modeling of parameterized multi-physics computations for the molten salt fast reactor, in: *Proc. of Int. Conf. on Mathematics and Computational Methods Applied to Nuclear Science and Engineering (M&C 2019)*, 2019, p. 10 pp.
  - [64] P. German, J. C. Ragusa, C. Fiorina, Application of multiphysics model order reduction to Doppler/neutronic feedback, *Nuclear Sci. Technol.* 5 (2019) 17.
  - [65] A. L. Alberti and T. S. Palmer, Reduced-order modeling of nuclear reactor kinetics using proper generalized decomposition, *Nuclear Science and Engineering* 194 (2020) 837–858.
  - [66] P. German, M. E. Tano, J. C. Ragusa, Reduced-order modeling of coupled neutronics and fluid dynamics in the zero-power molten salt fast reactor, in: *Proc. of Int. Conf. on Mathematics and Computational Methods Applied to Nuclear Science and Engineering (M&C 2021)*, 2021, p. 10 pp.
  - [67] R. Elzohery, J. Roberts, Modeling neutronic transients with galerkin projection onto a greedy-sampled, POD subspace, *Annals of Nuclear Energy* 162 (2021) 108–117.
  - [68] R. Elzohery, J. Roberts, Exploring transient, neutronic, reduced-order models using DMD/POD-Galerkin and data-driven DMD, *EPJ Web Conf.* 247 (2021) 15019.

- [69] R. Elzohery, J. Roberts, A multiphysics reduced-order model for neutronic transient using POD-Galerkin projection and DEIM, *Transactions of the American Nuclear Society* 125 (2021) 440–443.
- [70] T. R. F. Phillips, C. E. Heaney, B. S. Tollit, P. N. Smith, C. C. Pain, Reduced-order modelling with domain decomposition applied to multi-group neutron transport, *Energies* 14 (2021) 1369.
- [71] K. A. Dominesey, W. Ji, Reduced-order modeling of neutron transport separated in energy by proper generalized decomposition with applications to nuclear reactor physics, *Journal of Computational Physics* 449 (2022) 110744.
- [72] A. S. Moore, T. M. Guymer, J. Morton, B. Williams, J. L. Kline, N. Bazin, C. Bently, S. Allan, K. Brent, A. J. Comley, K. Flippo, J. Cowan, J. M. Taccetti, K. Missack-Tamashiro, D. W. Schmidt, C. E. Hamilton, K. Obrey, N. E. Lanier, J. B. Workman, R. M. Stevenson, Characterization of supersonic radiation waves, *Journal of Quantitative Spectroscopy & Radiative Transfer* 159 (2015) 19–28.
- [73] D. Anistratov, N. Stehle, Computational transport methodology based on decomposition of a problem domain into transport and diffusive subdomains, *Journal of Computational Physics* 231 (2012) 8009–8028.
- [74] N. Stehle, D. Anistratov, M. Adams, A hybrid transport-diffusion method for 2D transport problems with diffusive subdomains, *Journal of Computational Physics* 270 (2014) 325–344.
- [75] M. R. Krumholz, R. I. Klein, C. F. McKee, J. Bolstad, Equations and algorithms for mixed-frame flux-limited diffusion radiation hydrodynamics, *The Astrophysical Journal* 667 (2007) 626–643.
- [76] R. Kuiper, H. Klahr, C. Dullemond, W. Kley, T. Henning, Fast and accurate frequency-dependent radiation transport for hydrodynamics simulations in massive star formation, *Astronomy & Astrophysics* 511 (2010) A81.
- [77] M. González, N. Vaytet, B. Commerçon, J. Masson, Multigroup radiation hydrodynamics with flux-limited diffusion and adaptive mesh refinement, *Astronomy & Astrophysics* 578 (2015) A12.
- [78] H. Tetsu, T. Nakamoto, Comparison of implicit schemes to solve equations of radiation hydrodynamics with a flux-limited diffusion approximation: Newton-Raphson, operator splitting, and linearization, *The Astrophysical Journal Supplement Series* 223 (2016) 14.
- [79] G. N. Minerbo, Maximum entropy Eddington factors, *Journal of Quantitative Spectroscopy & Radiative Transfer* 20 (1978) 541–545.
- [80] B. Su, M. G. Fried, E. W. Larsen, Stability analysis of the variable Eddington factor method, *Transport Theory and Statistical Physics* 30 (2001) 439–455.
- [81] F. D. Swesty, E. S. Myra, A numerical algorithm for modeling multigroup neutrino-radiation hydrodynamics in two spatial dimensions, *The Astrophysical Journal Supplement Series* 181 (2009) 1–52.
- [82] M. A. Skinner, E. C. Ostriker, A two-moment radiation hydrodynamics module in Athena using a time-explicit Godunov method, *The Astrophysical Journal Supplement Series* 206 (2013) 21.
- [83] M. Klassen, R. Kuiper, R. E. Pudritz, T. Peters, R. Banerjee, L. Bunttemeyer, A general hybrid radiation transport scheme for star formation simulations on an adaptive grid, *The Astrophysical Journal* 797 (2014) 4.
- [84] W. Zhang, L. Howell, A. Almgren, A. Burrows, J. Dolence, J. Bell, CASTRO: A new compressible astrophysical solver. III. multigroup radiation hydrodynamics, *The Astrophysical Journal Supplement Series* 204 (2013) 7.
- [85] V. Ya. Gol’din, Characteristic difference scheme for non-stationary kinetic equation, *Soviet Mathematics Doklady* 1 (1960) 902–906.
- [86] K. Takeuchi, A numerical method for solving the neutron transport equation in finite cylindrical geometry, *Journal of Nuclear Science and Technology* 6 (1969) 446–473.
- [87] J. R. Askew, A characteristic formulation of the neutron transport equation in complicated geometries, Technical Report M1108, Atomic Energy Establishment, 1972.
- [88] H. D. Brough, C. T. Chudley, Characteristic ray solutions of the transport equation, in: J. Lewis, M. Becker (Eds.), *Advances in Nuclear Science and Technology*, volume 12, Plenum Press, 1980, pp. 1–30.
- [89] J. R. Askew, M. J. Roth, WIMS-E: A scheme for neutronics calculations, Technical Report AEEW-R-1315, United Kingdom Atomic Energy Authority, 1982.
- [90] M. Edenius, K. Ekberg, B. H. Forssén, D. Knott, CASMO-4, A fuel assembly burnup program, User’s

- manual, Studsvik/SOA-93/1, Studsvik of America, 1993.
- [91] M. Zika, M. Adams, Acceleration for long-characteristics assembly-level transport problems, *Nuclear Science and Engineering* 134 (2000) 135–158.
  - [92] J. M. Coale, D. Y. Anistratov, Multilevel method for thermal radiative transfer problems with method of long characteristics for the Boltzmann transport equation, in: *Proc. of Int. Conf. on Mathematics and Computational Methods Applied to Nuclear Science and Engineering (M&C 2023)*, Niagara Falls, Ontario, Canada, 2023, p. 10 pp.
  - [93] J. A. Fleck, J. D. Cummings, An implicit Monte Carlo scheme for calculating time and frequency dependent nonlinear radiation transport, *J. of Comp. Phys.* 8 (1971) 313–342.
  - [94] L. K. Abu-Shumays, Angular quadratures for improved transport computations, *Transport Theory & Statistical Physics* 30 (2001) 169–204.
  - [95] P. Ghassemi, D. Y. Anistratov, Multilevel quasidiffusion method with mixed-order time discretization for multigroup thermal radiative transfer problems, *Journal of Computational Physics* 409 (2020) 109315.
  - [96] T. M. Guymer, A. S. Moore, J. Morton, J. L. Kline, S. Allan, N. Bazin, J. Benstead, C. Bentley, A. J. Comley, J. Cowan, K. Flippo, W. Garbett, C. Hamilton, N. E. Lanier, K. Mussack, K. Obrey, L. Reed, D. W. Schmidt, R. M. Stevenson, J. M. Taccetti, J. Workman, Quantifying equation-of-state and opacity errors using integrated supersonic diffusive radiation flow experiments on the National Ignition Facility, *Physics of Plasmas* 22 (2015) 043303.
  - [97] C. L. Fryer, E. Dodd, W. Even, C. J. Fontes, C. Greeff, A. Hungerford, J. Kline, K. Mussack, I. Tregillis, J. B. Workman, J. Bernstead, T. M. Guymer, A. S. Moore and J. Morton, Uncertainties in radiation flow experiments, *High Energy Density Physics* 18 (2016) 45–54.
  - [98] C. L. Fryer, A. Diaw, C. J. Fontes, A. L. Hungerford, J. Kline, H. Johns, N. E. Lanier, S. Wood, T. Urbatsch, Designing radiation transport tests: Simulation-driven uncertainty-quantification of the COAX temperature diagnostic, *High Energy Density Physics* 35 (2020) 100738.